AD-A114 282   ROCHESTER UNIV NY DEPT OF CHEMISTRY   F/G 20/5
LASER-GENERATED ELECTRON EMISSION FROM SURFACES: EFFECT OF THE --ETC(U)
APR 82 J LIN, T F GEORGE   N00014-80-C-0472
UNCLASSIFIED TR-18   NL

1 OF 1
AD
A114282

END
DATE
FILMED
6-82
DTIC

(12)

OFFICE OF NAVAL RESEARCH

Contract N00014-80-C-0472

Task No. NR 056-749

TECHNICAL REPORT No. 18

Laser-Generated Electron Emission from Surfaces: Effect of the Pulse Shape on Temperature and Transient Phenomena

by

Jui-teng Lin and Thomas F. George

Prepared for Publication

in

Journal of Applied Physics

University of Rochester
Department of Chemistry
Rochester, New York 14627

April, 1982

Unclassified
SECURITY CLASSIFICATION OF THIS PAGE (When Data Entered)

REPORT DOCUMENTATION PAGE		READ INSTRUCTIONS BEFORE COMPLETING FORM
1. REPORT NUMBER 18	2. GOVT ACCESSION NO. AD-A114 28	3. RECIPIENT'S CATALOG NUMBER
4. TITLE (and Subtitle) Laser-Generated Electron Emission from Surfaces: Effect of the Pulse Shape on Temperature and Transient Phenomena		5. TYPE OF REPORT & PERIOD COVERED Interim Technical Report
		6. PERFORMING ORG. REPORT NUMBER
7. AUTHOR(s) Jui-teng Lin and Thomas F. George		8. CONTRACT OR GRANT NUMBER(s) N00014-80-C-0472
9. PERFORMING ORGANIZATION NAME AND ADDRESS University of Rochester Department of Chemistry Rochester, New York 14627		10. PROGRAM ELEMENT, PROJECT, TASK AREA & WORK UNIT NUMBERS NR 056-749
11. CONTROLLING OFFICE NAME AND ADDRESS Office of Naval Research Chemistry Program Code 472 Arlington, Virginia 22217		12. REPORT DATE April, 1982
		13. NUMBER OF PAGES 23
14. MONITORING AGENCY NAME & ADDRESS(if different from Controlling Office)		15. SECURITY CLASS. (of this report) Unclassified
		15a. DECLASSIFICATION/DOWNGRADING SCHEDULE

16. DISTRIBUTION STATEMENT (of this Report)

This document has been approved for public release and sale; its distribution is unlimited.

17. DISTRIBUTION STATEMENT (of the abstract entered in Block 20, if different from Report)

18. SUPPLEMENTARY NOTES

Prepared for publication in Journal of Applied Physics, in press.

19. KEY WORDS (Continue on reverse side if necessary and identify by block number)

LASER-SURFACE INTERACTIONS	LASER PULSE SHAPE
ELECTRON EMISSION	SURFACE TEMPERATURE
IONIZATION OF ADSPECIES	ELECTRON CURRENT PULSE
Cs/W ADSPECIES/SURFACE	GENERALIZED RICHARDSON EQUATION

20. ABSTRACT (Continue on reverse side if necessary and identify by block number)

Surface temperatures generated by gaussian, rectangular and triangular laser pulses are determined by solving a heat diffusion equation. The dependence of the temperature on the pulse shape, and in turn the dependence of the thermal diffusivity and absorbtance on the temperature, are investigated. The lifetime of an adspecies on a laser-heated solid e.g., Cs on W) is estimated in terms of the temperature, the desorption energy and the coverage. The mechanism of laser-generated electron emission from the adspecies is analyzed by means of the Richardson equation. A

Unclassified
SECURITY CLASSIFICATION OF THIS PAGE (When Data Entered)

condition for generating an intense electron beam is that the laser pulse duration and the rise time of the temperature must be less than the lifetime of the adspecies.

JOURNAL OF APPLIED PHYSICS, in press

Laser-Generated Electron Emission from Surfaces: Effect of the Pulse Shape on Temperature and Transient Phenomena

Jui-teng Lin* and Thomas F. George
Department of Chemistry
University of Rochester
Rochester, New York 14627

Surface temperatures generated by gaussian, rectangular and triangular laser pulses are determined by solving a heat diffusion equation. The dependence of the temperature on the pulse shape, and in turn the dependence of the thermal diffusivity and absorptance on the temperature, are investigated. The lifetime of an adspecies on a laser-heated solid (e.g., Cs on W) is estimated in terms of the temperature, the desorption energy and the coverage. The mechanism of laser-generated electron emission from the adspecies is analyzed by means of the Richardson equation. A condition for generating an intense electron beam is that the laser pulse duration and the rise time of the temperature must be less than the lifetime of the adspecies.

I. Introduction

Laser transient effects in the areas of surface physics and materials science have been recently investigated, and surface-related phenomena such as annealing, vaporization, ionization, dissociation and adsorption have received considerable attention, both experimentally and theoretically, due to their potential importance in applications to microelectronics,[1] heterogeneous rate processes,[2] nondestructive materials testing[3] and new laser developments.

One of the important laser transient effects is the electron current emitted from low work function materials. The extent to which the current can be regarded as "photoelectric" or "thermionic" has not yet been conclusively determined, due to the complexity of the various competing transient phenomena (e.g., desorption and migration) and to the lack of understanding as to how such phenomena are related to the coherence of the laser radiation and the thermal and optical properties of the solid. From Richardson's equation it is seen that the thermionic current is governed mainly by the work function and the surface temperature of the laser-heated solid.[4] There is a time delay in the maximum surface temperature and hence the current with respect to the peak laser intensity. The electron emission spectrum is also dependent on the length and overall shape of the laser pulse. We have therefore decided to analyze the effects of the laser pulse shape on the surface temperature and its time delay. By using a generalized Richardson equation, we are able to incorporate the conditions and processes leading to both thermionic and photoelectric currents.

In this paper we present some theoretical aspects of laser-generated electron emission from low work function materials, e.g., a cesiated tungsten surface. By solving the heat diffusion equation, we are able to analyze the effect of the pulse shape on the temperature and its time delay. In this regard, in Section II we compare the surface temperatures generated by gaussian, rectangular and triangular pulses. In Section III, the laser-generated electron emission is analyzed by means of a generalized Richardson equation. While the main focus is on the thermionic current, photoelectric effects are discussed for a cesiated tungsten surface. The diffusion equation with temperature-dependent diffusivity and absorptance is solved in Section IV. Finally, the desorption mechanism and the residence time of the adspecies are discussed in Section V.

II. Surface Temperature: Effects of the Pulse Shape and Time Delay

For a heterogeneous system, e.g., Cs/W, subjected to laser radiation, the photon energy can be absorbed by both the adspecies and the substrate. However, the main absorption is by the adspecies, and we therefore will be interested in the temperature associated with just the surface formed by the adspecies. To begin, let us consider the laser-generated transient temperature, $T(z,t)$, which depends on time and the surface depth z and corresponds to the above surface temperature at $z = 0$. This obeys the heat diffusion equation[5]

$$\frac{\partial T}{\partial t} = D\frac{\partial^2 T}{\partial z^2} , \tag{1.a}$$

with the initial and boundary conditions

$$T(r,z,0)=T_0 , \tag{1.b}$$

$$K\frac{\partial T}{\partial z}\bigg|_{z=0} = -\ (1-R)I(r,z,t)\big|_{z=0} . \tag{1.c}$$

$T(r,z,t)$ is the laser irradiated target temperature with hot spot centered at $r = 0$ and surface reflectivity R (at $z = 0$); D is the thermal diffusivity related to the specific heat (c), the mass density (ρ) and the thermal conductivity (K) by $D = K/\rho c$; and I represents the incident laser pulse in terms of a spatial gaussian dependence and a temporal dependence $g(t)$ as

$$I(r,0,t) = I_0 \exp[-(r/d)^2] g(t). \tag{2}$$

We shall first consider the case where both the thermal and optical coefficients are temperature independent and shall restrict ourselves to times satisfying the condition $d >> (4Dt)^{1/2}$, such that thermal diffusion effects in the radial (r) direction are negligible. Although the above procedure is valid only for surface heat generation, it gives satisfactory results for volume heat generation provided the laser intensity is less than 100 MW/cm^2 and the pulse length is greater than a nanosecond.[6] The rigorous procedure for volume heat generation applies to arbitrary intensity and pulse length. In this case the boundary condition is

$$K(\partial T/\partial z)_{z=0} = 0, \tag{3.a}$$

where the diffusion equation is

$$\partial T/\partial t = D(\partial^2 T/\partial z^2) + S(r,z,t), \tag{3.b}$$

with the radiation heat source given as

$$S = (\beta/\rho c) I_0 (1-R) \exp(-\beta z) g(t), \tag{3.c}$$

and β is the absorption coefficient. Hence, for the case of a very high-power short-pulse heating source, e.g., gigawatt picosecond laser, we shall rely on volume heat generation for calculating the transient temperature [which would be overestimated by Eq. (1).][6] The solution of Eq. (3) for volume heat generation is considerably more complicated than that of Eq. (1) for surface heat generation due to the z-dependent heat source $S(r,z,t)$. However, for our systems of interest the laser intensity is low enough and the pulse duration long enough for Eq. (1) to be valid, which we shall solve below.

Using Eq. (1), we shall now analyze the effect of the laser pulse shape on the maximum surface temperature and its time delay, which in turn gives the time delay of the electron current. By employing the Green's function technique, we obtain an integral expression for the surface temperature, i.e., solution of the diffusion equation at $z = 0$,[5]

$$T_s(r,0,t) = T_0 + \frac{I_0(1-R)}{(\pi K\rho c)^{1/2}} \exp\left[-\left(\frac{r}{d}\right)^2\right] \int_{-\infty}^{t} g(t-t')/(t')^{1/2}\,dt' \qquad (4)$$

For an arbitrary laser pulse shape, the above integration must be carried out numerically. For the case of a rectangular pulse with constant intensity I_0 and duration t_p, the integration can be performed analytically. This yields an expression for the maximum surface temperature $T_s = 2I_0(1-R)t_p^{1/2}/(\pi K\rho c)^{1/2}$, which, however, tends to overestimate actual experimental results. We therefore propose triangular pulses to better approximate an actual pulse, e.g., a gaussian or an asymmetric long-tail pulse. The effect of the triangular pulse shape on the temperature and its time delay can be analyzed by means of an exact analytic solution of the diffusion equation.

A triangular temporal dependence of the laser pulse takes the form

$$g(t) = I_0 t/a, \qquad 0 \leq t \leq a \tag{5.a}$$

$$= I_0(a+b-t)/b\ , \qquad a \leq t \leq a+b \tag{5.b}$$

$$= 0\ , \qquad \text{otherwise}, \tag{5.c}$$

which has a peak intensity at $t = t_1^* = a$ with a pulse energy $(a+b)I_0/2$, and whose shape is governed by the ratio between a and b. From Eq.(4), the surface temperature generated by the above triangular pulse can be given exactly, in the form

$$T_s(r,0,t) = T_0 + B(r)\,I_0\,T_1(t)\ , \qquad 0 \leq t \leq b \tag{6.a}$$

$$= T_0 + B(r)\,I_0 \sum_{i=1}^{3} T_i(t)\ , \qquad a \leq t \leq a+b \tag{6.b}$$

$$= T_0 + B(r)I_0 \sum_{i=1}^{4} T_i(4)\ , \qquad a+b \leq t \tag{6.c}$$

where $B(r) = (1-R)\exp[-(r/d)^2]/(\pi K\rho c)^{1/2}$ and

$$T_1(t) = 4t^{3/2}/3a\ , \tag{7.a}$$

$$T_2(t) = -2(t-a)^{1/2}(2t+a)/3a\ , \tag{7.b}$$

$$T_3(t) = 2(t-a)^{1/2} - 4(t-a)^{3/2}/3b\ , \tag{7.c}$$

$$T_4(t) = 4(t-a-b)^{3/2}/3b\ . \tag{7.d}$$

By setting $[\partial T_s(r,0,t)/\partial t]_{t=t_2^*} = 0$ we obtain the rise time for the maximum surface temperature, $t_2^* = aL^2/(L^2-1)$, which then gives us the delay time by means of the simple expression

$$\Delta t = t_2^* - t_1^* = a/(L^2-1)\ , \tag{8}$$

where L = (a+b)/b and $t_1^* = a$ is the rise time of the peak laser intensity.

To show the effect of the pulse shape on the surface temperature, we plot the analytical results for the rectangular and triangular pulses and the numerical result for a gaussian pulse (with FWHM = 18.8 ns) in Fig. 1. It is seen that when the laser pulse is gaussian, the surface temperature is overestimated by a rectangular pulse but is well approximated by a triangular pulse with equal sides (a=b). Note that in the surface temperature profiles (shown in Fig. 1) the laser energies ($\int g(t)dt$) of different pulses are all the same, and the surface temperatures are normalized to the maximum value generated by a rectangular pulse.

By knowing the rise time of the maximum surface temperature, t_2^*, we can easily calculate the maximum surface temperature for different triangular pulse shapes from Eq. (6). Fig. 2 shows the delay time and the maximum surface temperature as a function of the value of a. The results suggest that a right-triangular pulse (with b = 0) generates higher temperature than that of the other shapes with b > 0.

III. Mechanism of Laser-Generated Electron Emission

Laser-generated electron emission of solids has been studied during the past several years.[7,8,9] There has been some recent discussion on two different emission mechanisms - photoelectric effect and thermionic emission - based on the reported experimental results.[10,11,12] However, no conclusive interpretation has been made due to the complexity of the transient phenomena. The mechanism of the electron emission depends on both the coherence properties of the incident laser radiation and the thermal/optical properties of the heated materials. The former includes intensity, polarization and frequency, and the latter includes the bond structure.

In order to characterize the electron emission with respect to the above, we utilize the generalized Richardson equation for the current density,[4,9,13,14]

$$J = \sum_{n=0}^{N+1} J_n , \tag{9}$$

with

$$J_n = a_n I_0^n A(1-R)^n T_s^2 F(\delta) . \tag{10}$$

J_n represents pure thermionic emission for $n = 0$ and the n-photon photoelectric effects for $n > 0$; A and a_n are the Richardson constant and the appropriate coefficient related to the matrix element of quantum n-photon processes, respectively; $F(\delta)$ is the Fowler function with the argument $\delta = nh\nu - \phi$, where $h\nu$ and ϕ are the photon energy and system work function, respectively. Here we sum over all integers from $n = 0$ to $N+1$, N being the largest integer less than $\phi/h\nu$.

For a low work function material, e.g., a cesiated tungsten surface with $\phi \approx 2.0$ eV subjected to pulsed laser radiation with intensity $I_0 \approx 50$ MW/cm^2 and photon energy $h\nu = 1.165$ eV, we may use limiting forms of the Fowler function, for surface temperature $T_s < 2000$ K. This results in the following expression for the total current density from pure thermionic emission and from one- and two-photon photoelectric effects:

$$J = J_0 + J_1 + J_2 , \tag{11}$$

with

$$J_0 = a_0 A T_s^2 \exp(-\phi/kT_s) , \tag{12}$$

$$J_1 = (a_1/a_0)I_0(1-R)J_0 \exp(-h\nu/kT_s), \qquad (13)$$

$$J_2 = a_2AI_0^2(1-R)^2 \left[(2h\nu-\phi)^2/4k^2 + \left(\frac{\pi}{6} - e^{-\delta} \right) T_s^2 \right]. \qquad (14)$$

The above equations are valid for a material with low work function or low ionization energy, and hence are more applicable to metal adspecies rather than nonmetal adspecies. Note that, from the expression in Eq.(13), the one-photon emission current density J_1 is equivalent to that of the pure thermionic emission J_0 enhanced by a factor $a_1I_0\exp(h\nu/kT_s)$, which is photon energy and intensity dependent. For the two-photon process, the current density J_2 is independent of T_s provided T_s is sufficiently low, where the "cold" electrons generated by two-photon ionization dominate the current density. At sufficiently high surface temperatures, we expect the pure thermionic effect to be the major component of the total current density, and a much higher power law for the intensity dependence, $J(t) = J_0I^m(t)$, is expected. This power law provides information about the shape of the emitted current. For example, a gaussian laser intensity, $I(t) = I_0\exp(-t^2/B^2)$, gives a gaussian current density, $J(t) = J_0\exp(-t^2/\beta^2)$, with a narrower width $\beta = B/\sqrt{m}$ if it follows the power law. In general, we expect an intensity-dependent exponent, m, due to the mixture of pure thermionic emission and multiphoton ionization.

Fig. 3 shows the surface temperature (normalized to its peak value) generated by a gaussian laser pulse (at the hot spot center) and also shows the corresponding current density (only the pure thermionic current is plotted). We note that the surface temperature and the associated current profiles may be well approximated by the results generated by a triangular pulse with a = b in Eq.(6), which gives the peak surface temperature $T_s^* \propto I_0(a+b)^{1/2}$. Furthermore, the numerical results show that these profiles are universal for gaussian pulses with arbitrary laser intensity. The term "universal" implies that two gaussian pulses, with intensities and pulse durations related by $I_1/I_2 = (t_2/t_1)^{1/2}$, will generate the same surface and current density profiles when the appropriate time scales are chosen. For example, the profiles shown in Fig. 3(A) and (B) also describe those profiles generated by picosecond pulses with (intensity, FWHM) = (1.825 GW/cm^2, 15 ps) and (1.581 GW/cm^2, 20 ps), respectively. We note that a narrow width of the current density profile is generated by a short laser pulse. This is an important feature of laser-generated electron emission, in that one can generate an intense electron beam on a nanosecond (picosecond) time scale by a nanosecond (picosecond) laser pulse.

Since the power density in the laser beam is not spatially uniform, we expect the generated current density J(r,t) to be not only time dependent but also radially dependent on the heated surface. Therefore, it is appropriate to deal with the average emission per unit area (with hot spot radius d),

$$\bar{J}_0(t) = \frac{1}{\pi d^2}\int_0^d AT_s^2(r,t)\exp[-\phi/kT_s(r,t)]\,2\pi r dr, \tag{15}$$

where $T_s(r,t)$ is the surface temperature with r = 0 defining the hot spot center. For a spatially gaussian pulse, $T_s(r,t) = T_s(0)\exp(-r^2/d^2)$, the average current density becomes

$$\bar{J}_0(t) = \frac{AT_s^2(0)}{2}\left\{e^{-1}(W-e^{-1})e^{-We} + (1-W)e^{-W} + W^2\int_1^e y^{-1}e^{-Wy}dy\right\}, \tag{16}$$

where $W = \phi/kT_s(0)$. The last integral term can also be expressed by the exponential integral function $W^2[E_i(W) - E_i(We)]$. We note that the apparent average temperature $(\overline{T}_a)$ defined by $\overline{J}_0 = A\overline{T}_a^2\exp(-\phi/\overline{T}_a)$ is higher than the true average surface temperature $\overline{T}_t = T_s(0)(1-e^{-1})$.

IV. Temperature-Dependent Absorptance and Diffusivity

In Section II we have assumed both the thermal and optical absorption coefficients to be independent of the temperature, whereby the diffusion equation is analytically solvable, for example, by the Green's function technique. In the case of temperature-dependent thermal diffusivity and optical absorptance, we can solve the nonlinear diffusion equation numerically by transforming it into a set of difference equations.[15] In this section, however, we present some analytic methods which allow us to study the effect of the temperature dependence of the thermal and optical coefficients.

Let us first allow the absorptance $\alpha=1-R$ to be temperature dependent while keeping the diffusivity constant. The boundary condition in Eq.(3.a) becomes

$$K\left(\frac{\partial T}{\partial z}\right)_{z=0} = -\alpha(T)I(z,t). \tag{17}$$

Taking the Laplace transform of the time variable in the above boundary condition and the diffusion equation and letting $\overline{T}(u)$ denote the Laplace transform of the surface temperature $T_s(t)$, then with the initial condition $T(z,0) = 0$ we obtain

$$u\overline{T}(u) = D\frac{\partial^2\overline{T}(u)}{\partial z^2}, \tag{18}$$

$$K\left(\frac{\partial \overline{T}(s)}{\partial z}\right)_{z=0} = \mathcal{L}[\alpha(T)I(z,t)], \tag{19}$$

where $\mathcal{L}$ denotes the Laplace transform. Multiplying Eq. (18) by $\exp[-(u/D)^{1/2}z]$ and performing the integration by parts, we obtain, in combining with Eq.(19), the surface temperature by means of the inverse Laplace transform:

$$\bar{T}(u) = (Kc\rho u)^{-1/2}\mathcal{L}(\alpha(T)I(z,t)] . \tag{20}$$

$$T_s(t) = \mathcal{L}^{-1}[\bar{T}(u)\} . \tag{21}$$

In principle, for arbitrary forms of the optical absorptance and the laser intensity, we can find the corresponding surface temperature by Eqs.(20) and (21). However, difficulties can arise in finding the inverse Laplace transforms. For tractable results, let us consider a linearly temperature-dependent absorptance, which is appropriate for most metallic surfaces, and assume a constant intensity, i.e. $\alpha(T) = A_0 + A_1T_s(t)$ and $I(t) = I_0$. Eq.(20) then gives[16]

$$\bar{T}(u) = A_0I_0/[u(Kc\rho u)^{1/2} - A_1I_0u] . \tag{22}$$

The inverse Laplace transform leads to the surface temperature[17]

$$T_s(t) = \frac{A_0}{A_1}\{[1+\mathrm{erf}(Xt)]\exp[(Xt)^2] - 1\} , \tag{23}$$

or

$$T_s(t) = \frac{A_0I_0}{\sqrt{Kc\rho}} \sum_{n=3}^{\infty} \frac{t^{n/2-1}X^{n-3}}{\Gamma(n/2)} , \tag{24}$$

where $X = A_1I_0/(Kc\rho)^{1/2}$, and erf(Xt) and $\Gamma(n/2)$ are the error and gamma functions, respectively. The leading term in Eq.(24) represents the surface temperature for $A_1 = 0$ (constant absorptance), and the remaining terms represent the contribution from the temperature dependence of $\alpha(T)$. It is seen that the error resulting from neglecting the temperature dependence of $\alpha(T)$ is large when the series in Eq.(24) is not rapidly convergent, which is the case for high-power/energy laser heating of metallic surfaces. This is one of the major concerns in high-power laser-damage studies. However, in laser-generated electron emission from a tungsten surface (with a rather high absorptance $\approx 40\%$), the temperature dependence of $\alpha(T)$ can be treated as a small correction compared with that of other metallic surfaces, e.g., with silver for which the absorptance is low ($\approx 2\%$) and $\alpha(T)$ is strongly temperature dependent.

We next consider the situation where both D and α are temperature dependent. For tractable results, we again consider the case where $\alpha = A_0 + A_1 T_s(t)$ and $I(t) = I_0$. Within the time scale $4\alpha^2 DT \gg 1$, the surface temperature follows the power law

$$T_s(t) = \frac{2I_0A_0}{\sqrt{\pi}\rho c}(t/D_0)^{1/2} \qquad (25)$$

for a constant $D = D_0$ and absorptance $\alpha = A_0$. When D is temperature dependent, the diffusion equation can be solved by, e.g., a Boltzmann transformation[5] with $\alpha = A_0$. The temperature follows the power law[5] $T_s(t) \propto t^{1/(m-2)}$ for $D(T) = D_0 T_s^m$. For weak temperature dependence of the thermal and optical absorption coefficients, we may use an iterative or adiabatic approximation to obtain the temperature power law by expressing α and D as $\alpha(T) = A_0 + A_1 T_s(t)$ and $D(T) = D_0/[1+ D_1 T_s(t)]$. The surface temperature then to first order in α and zeroth order in D is given by [from Eq.(24)]

$$T_s(t) = \frac{A_0 I_0}{c\rho}[2(t/\pi D_0)^{1/2} + A_1 I_0 t/(\rho c D_0)] \ . \qquad (26)$$

The next higher-order surface temperature, neglecting terms like A_1D_1, etc., is found to be

$$T_s(t) = Z_1 + (Z_1^2 + Z_0)^{1/2} \quad , \tag{27}$$

where

$$Z_0 = \left(\frac{A_0I_0^2t}{K(\rho c)^2\pi}\right)\left[\frac{4A_0}{D_0} - \frac{\pi}{(D_0\rho c)^2}A_1I_0t\right] \quad , \tag{28.a}$$

$$Z_1 = \left(\frac{1}{2D_0}\right)\left(\frac{A_0I_0^2t}{\sqrt{K}(\rho c)^2\pi}\right)(\pi A_1+4A_0D_1) \quad . \tag{28.b}$$

When the pulse energy and the intensity are sufficiently high, the surface temperature power law becomes $T_s(t) \propto I_0^2t$, in contrast to the constant-coefficients limit (A_1=D_1=0) where the power law is $T_s(t) \propto I_0t^{1/2}$.

V. Effects of Laser-Stimulated Surface Processes

It is known that in a heterogeneous system with species adsorbed (chemically or physically) on a substrate surface, laser radiation not only causes nonselective thermal effects but also selective quantum effects.[18] Laser-stimulated surface processes such as migration (diffusion), desorption (evaporation) and dissociation (decomposition) will affect the thermionic and photoelectric current through the electron emission characteristics, e.g., the coverage-dependent work function, binding energy and the temperature-dependent residence time of the low work function adspecies.

An important factor in a laser-generated high-intensity electron beam from a low work function surface is the lifetime (residence time) of the adspecies. In general, the adspecies total lifetime

(τ) may be related to the desorption rates W_i by

$$\tau^{-1} = \sum_i W_i(T_s, E_A, \theta) . \tag{29}$$

The desorption rates depend on the surface temperature (T_s), the activation energy (E_A), the adspecies coverage (θ) and the thermal and optical properties of the material, and the subscript i designates a particular process such as: (1) migration-induced desorption, (2) thermal-phonon-enhanced desorption, (3) ionization-induced bond breaking and (4) direct laser-induced bond breaking (or selective desorption).[19-21]

An accurate estimation of the lifetime including all the possible desorption mechanisms is a difficult task. For example, to obtain the phonon-induced desorption rate, we must calculate matrix elements of the phonon interaction Hamiltonian using wavefunctions based on an actual surface bond potential.[22] To obtain the direct laser-induced bond breaking rate, we must solve the generalized master equation in energy space[2] and then find the desorption rate by employing, for example, Slater's unimolecular theory.[23] For a rough estimation of the lifetime, one can assume a simple Arrhenius form for the lifetime,[24]

$$\tau^{-1} = k_0 \exp\{-[E_d - F(\theta)]/kT\} , \tag{30}$$

where k_0 is a preexponential factor ($10^{12} \sim 10^{13}$ sec^{-1}), E_d is the desorption energy given by the bond strength of the adspecies and $F(\theta)$ is a coverage-dependent correction factor for the adspecies-adspecies interaction. The lifetime of an adsorbed cesium atom with $E_d = 2.05$ eV is about 150 ns for a tungsten surface heated to 2000 K (assuming $F(\theta)\simeq 0$). Due to the long lifetime, the work function of the surface is essentially "frozen" at a low value ($\phi \simeq$ 2eV) during the pulse period, where the cesium remains adsorbed on the metallic surface and in thermal equilibrium with the surface phonons.

In conclusion, we propose some possible procedures to aid in the development of high-quality electron beams via laser-activated low work function materials:

(1) Increase the peak value of the laser-induced surface temperature by choosing an appropriate pulse shape, e.g., a right-triangular pulse.

(2) Optimize the thermal and optical parameters of the heated material such as the work function, diffusivity, melting temperature, reflectivity (absorptance), ionization energy, etc.

(3) Increase the thermal stability of the adspecies, e.g., by the co-adsorption of oxygen on a cesiated tungsten surface in which the layer of cesium oxide can have a work function ($\simeq$1.0 eV) lower than that of cesium itself ($\simeq$2.0 eV).[25,26]

Acknowledgments

We would like to thank Drs. E. J. Britt and B. C. F. M. Laskowski for useful discussions on the experimental aspects of laser-generated coherent electrons and Dr. P. E. Oettinger for sending us a report on laser-activated surface electron emission prior to publication.[27] This work was supported in part by the Office of Naval Research and the Air Force Office of Scientific Research (AFSC), United States Air Force, under Grant AFOSR 82-0046. The United States Government is authorized to reproduce and distribute reprints for governmental purposes nothwithstanding any copyright notation hereon. TFG acknowledges the Camille and Henry Dreyfus Foundation for a Teacher-Scholar Award (1975-82).

* Also affiliated with the Laboratory for Laser Energetics, University of Rochester, Rochester, New York 14623.

References

1. S. D. Ferris, H. J. Leamy and J. M. Poate, Eds., Laser-solid Interactions and Laser Processing (AIP, New York, 1979); C. W. White and P. S. Peersey, Eds., Laser and Electron Beam Processing of Materials (Academic Press, New York, 1980).
2. J. Lin and T. F. George, Chem. Phys. Lett. **66**, 5 (1979).
3. R. J. von Gutfeld and R. L. Melcher, Materials Evaluation **35**, 97 (1977); R. J. von Gutfeld and S. S. Wang, IBM Tech. Discl. Bull. **21**, 3441 (1979).
4. R. H. Fowler, Phys. Rev. **38**, 45 (1931).
5. H. S. Carslaw and J. C. Jaeger, Conduction of Heat in Solids, 2nd Ed. (Oxford U.P., London, 1959); M. N. Ozisik, Boundary Value Problems in Heat Conduction (International Textbook Co., Scranton, 1968); J. F. Ready, Effects of High Power Laser Radiation (Academic Press, New York, 1971).
6. J. H. Bechtel, J. Appl. Phys. **46**, 1585 (1975).
7. J. F. Ready, Phys. Rev. **137**, A620 (1965); J. Appl. Phys. **36**, 462 (1965); W. L. Knecht, Appl. Phys. Lett. **6**, 99 (1965).
8. E. M. Logothetis and P. L. Hartman, Phys. Rev. **187**, 460 (1969).
9. J. H. Bechtel, W. L. Smith and N. Bloembergen, Opt. Commun. **13**, 56 (1975).
10. U. A. Arifov, V. V. Kazanskii, V. B. Logovskoi and V. A. Makarenko, Sov. Phys. Tech. Phys. **21**, 239 (1976); **24**, 238 (1979).
11. U. A. Arifov, V. B. Lugovskoi and V. A. Makarenko, Sov. Phys. Solid State **20**, 867 (1978).
12. E. Ya. Zandberg, E. G. Nazarov and U. Kh. Rasulev, Sov. Phys. Tech. Phys. **25**, 1024 (1980).

13. R. K. Pathria, *Statistical Mechanics* (Pergamon, New York, 1972), Ch. 8.

14. M. E. Marinchuk, Phys. Lett. **34A**, 97 (1971); I. I. Kantorovich, Sov. Phys. Tech. Phys. **22**, 397 (1977).

15. J. R. Ockendon and W. R. Hodgkins, Eds., *Moving Boundary Problems in Heat Flow and Diffusion* (Clarendon Press, Oxford, 1974).

16. A. E. Rosenbluth, private communication (1976).

17. F. Oberhettinger and L. Badii, *Tables of Laplace Transforms* (Springer-Verlag, New York, 1973).

18. J. Lin and T. F. George, Surface Sci. **100**, 381 (1980).

19. J. Lin and T. F. George, J. Chem. Phys. **72**, 2554 (1980).

20. T. F. George, J. Lin, K. S. Lam and C. Chang, Opt. Eng. **19**, 100 (1980).

21. T. F. George, A. C. Beri, K. S. Lam and J. Lin, in *Laser Applications*, Vol. 5, R. K. Erf and J. F. Ready, Eds. (Academic Press, New York, 1982), in press.

22. B. Bendow and S.-C. Ying, Phys. Rev. B **7**, 622 (1973).

23. J. Lin and T. F. George, unpublished.

24. F. C. Tompkins, *Chemisorption of Gases on Metals* (Academic Press, New York, 1978), Chapters 5.3 and 9.2.

25. C. A. Papageorgopoulos and J. M. Chen, Surface Sci **39**, 313 (1973); J. L. Desplat, Surface Sci. **34**, 588 (1973).

26. E. V. Kiimenko and A. G. Naumovets, Sov. Phys. Tech. Phys. **24**, 710 (1979) and references therein.

27. C. Lee and P. E. Oettinger, Appl. Surface Sci. **8**, 206 (1981).

Figure Captions

Fig. 1. Normalized surface temperature profiles (T_s/T_s^*) for rectangular (solid line ——), gaussian (dotted line...) and triangular pulses with a = b/3 (dash-dot-dashed-··-), a = b (dashed ---) and a = 3b (dash-dot-dot-dashed -···-). $T_s^* \propto I_0 t_p^{1/2}$ is the maximum surface surface temperature generated by a rectangular pulse with duration t_p = 20 ns. The intensity profiles g(t) are also shown, where the guassian pulse has a FWHM = 18.8 ns and all pulses with different shapes have the same energy $I_0 t_p$.

Fig. 2. The normalized maximum surface temperature (T_s^*/T_R^*) and the time delay (Δt) as a function of the pulse shape factor a, for triangular pulses with bottom length a + b = 40 ns and energy $I_0(a+b)/2$. Note that the pulse shape factor governs the pulse shapes, e.g., a=40 and b=0 for right triangles and a = b = 20 for isosceles. The maximum surface temperature generated by a right triangle (with b = 0) is given by $T_R^* = [(1-R)/(\pi K \rho c)^{1/2}](4I_0/3)a^{1/2}$.

Fig. 3. The normalized surface temperature and current density (J/J*) as a function of time generated by gaussian pulses for [intensity(MW/cm^2), FWHM(ns)] = (A)(57.73,15), (B)(50,20), (C)(40.82,30) and (D)(35.35,40). Note that all of these pulses have the same peak surface temperature T_s^*, which is well approximated by $T_s^* = [(1-R)/(\pi K \rho c)^{1/2}] I_0 (2/\sqrt{3})^3 a^{1/2}$, as in the case for an isosceles triangle.

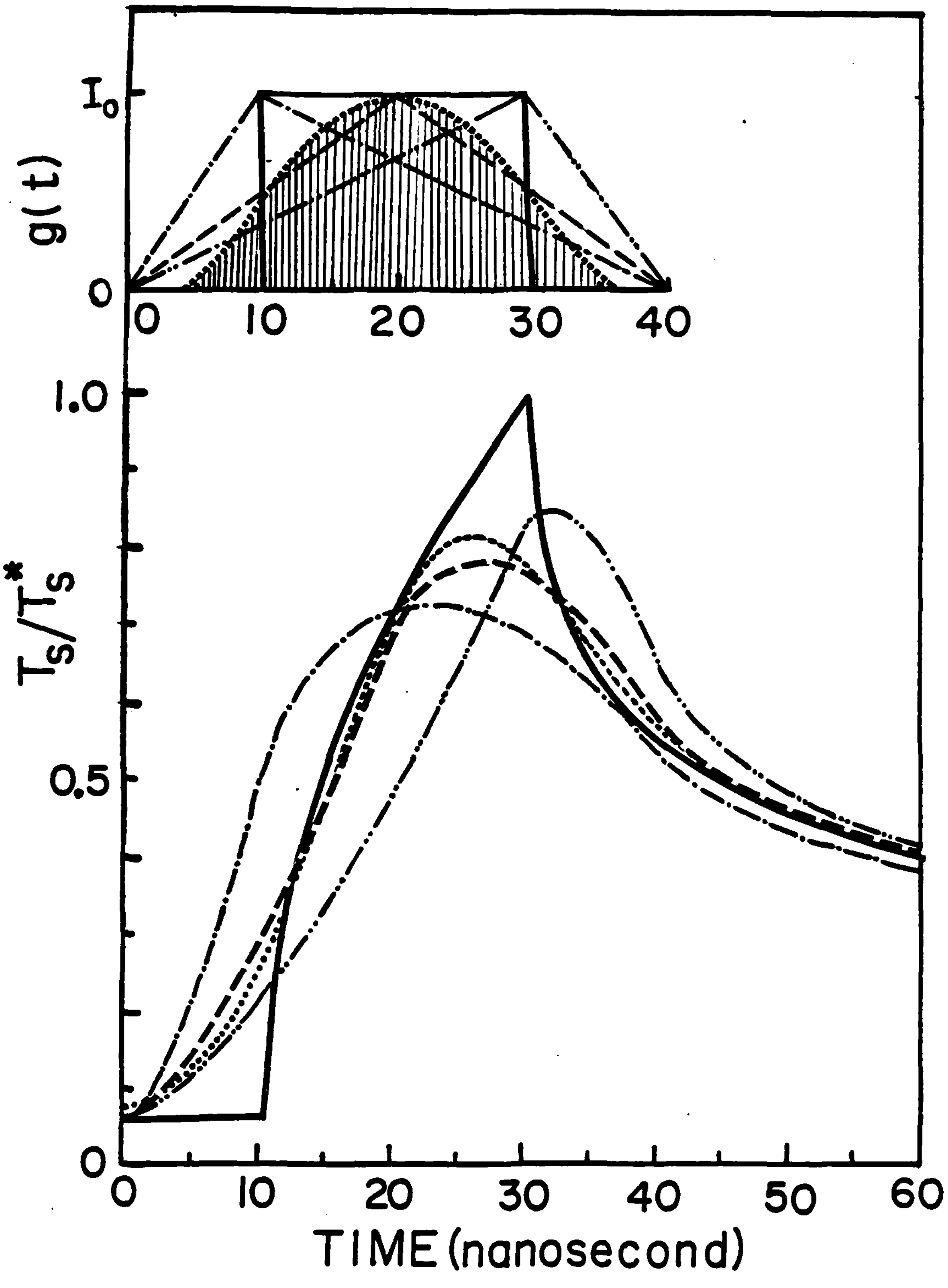
g(t)
I₀
0
0
10
20
30
40
T_s/T_s^*
1.0
0.5
0
0
10
20
30
40
50
60
TIME (nanosecond)

figure 1.

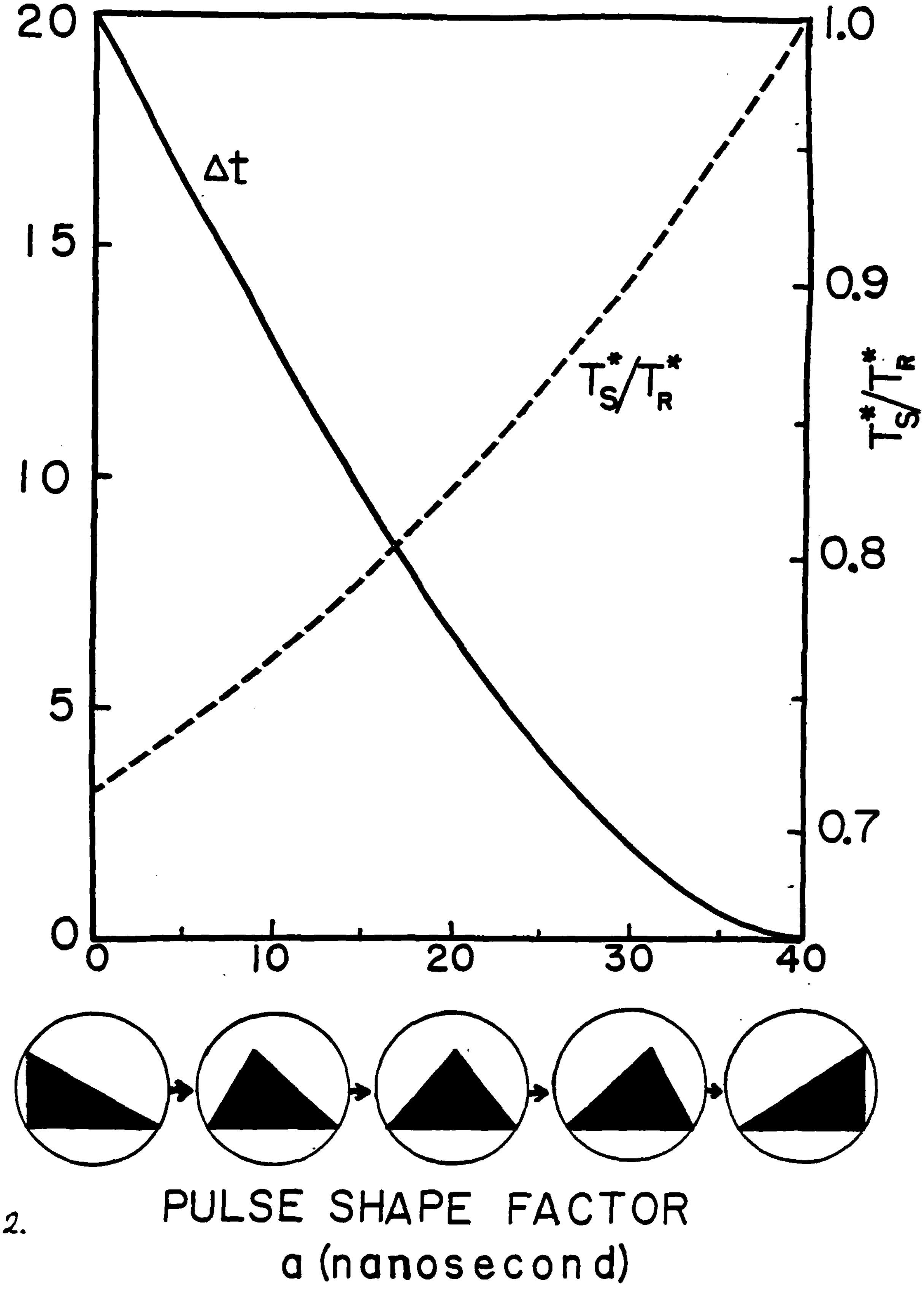
20
15
10
5
0
Δt (nanosecond)
1.0
0.9
0.8
0.7
T_S^*/T_R^*
Δt
T_S^*/T_R^*
0
10
20
30
40
PULSE SHAPE FACTOR
a (nanosecond)

figure 2.

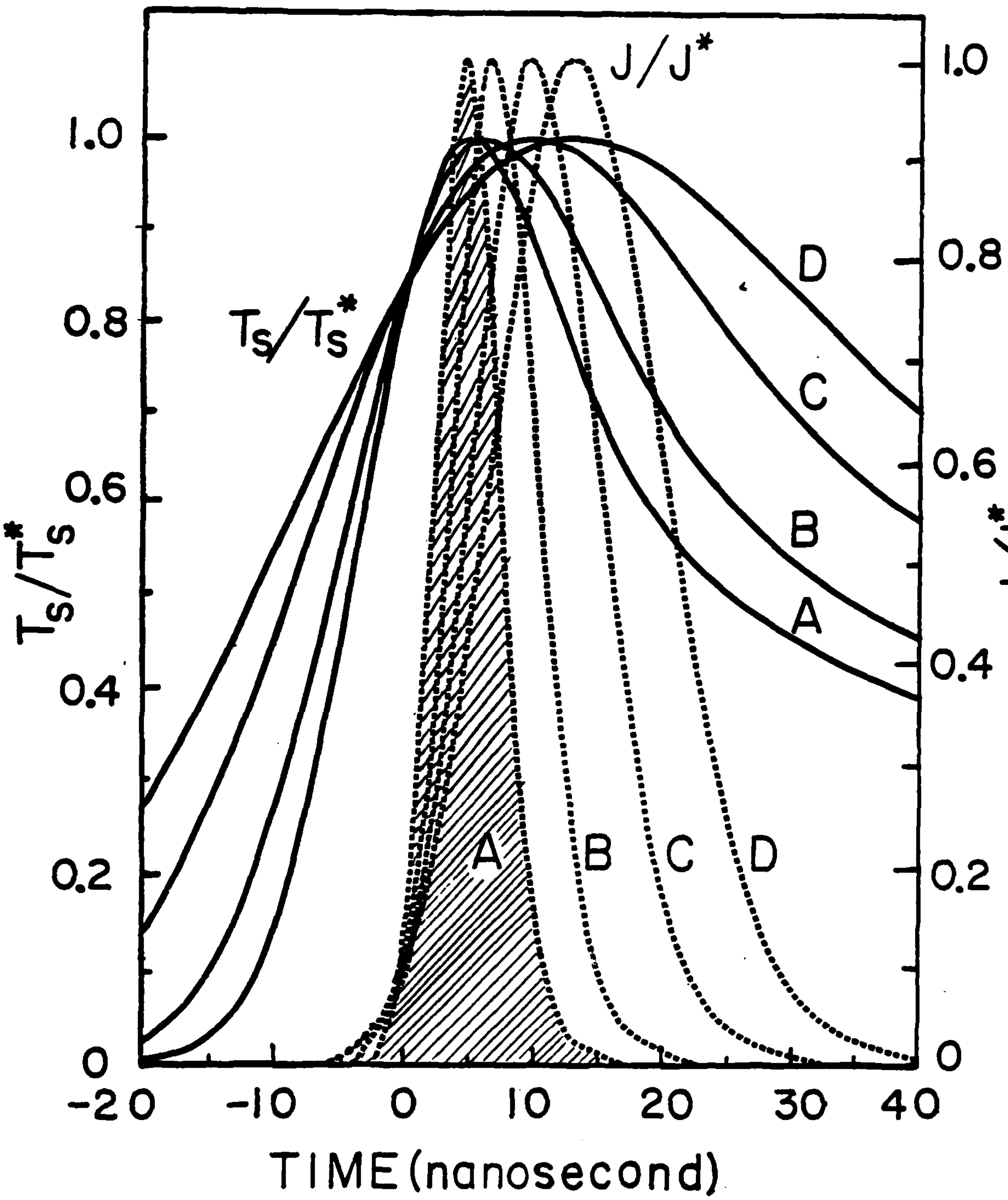
J/J*
1.0
0.8
0.6
0.4
0.2
0
1.0
0.8
0.6
0.4
0.2
0
Ts/Ts*
Ts/Ts*
J/J*
D
C
B
A
A
B
C
D
-20
-10
0
10
20
30
40
TIME (nanosecond)

figure 3.

TECHNICAL REPORT DISTRIBUTION LIST, GEN

No. Copies

Office of Naval Research
Attn: Code 472
800 North Quincy Street
Arlington, Virginia 22217 2

ONR Western Regional Office
Attn: Dr. R. J. Marcus
1030 East Green Street
Pasadena, California 91106 1

ONR Eastern Regional Office
Attn: Dr. L. H. Peebles
Building 114, Section D
666 Summer Street
Boston, Massachusetts 02210 1

Director, Naval Research Laboratory
Attn: Code 6100
Washington, D.C. 20390 1

The Assistant Secretary
of the Navy (RE&S)
Department of the Navy
Room 4E736, Pentagon
Washington, D.C. 20350 1

Commander, Naval Air Systems Command
Attn: Code 310C (H. Rosenwasser)
Department of the Navy
Washington, D.C. 20360 1

Defense Technical Information Center
Building 5, Cameron Station
Alexandria, Virginia 22314 12

Dr. Fred Saalfeld
Chemistry Division, Code 6100
Naval Research Laboratory
Washington, D.C. 20375 1

Dr. David L. Nelson
Chemistry Program
Office of Naval Research
800 North Quincy Street
Arlington, Virginia 22217 1

No. Copies

U.S. Army Research Office
Attn: CRD-AA-IP
P.O. Box 12211
Research Triangle Park, N.C. 27709 1

Naval Ocean Systems Center
Attn: Mr. Joe McCartney
San Diego, California 92152 1

Naval Weapons Center
Attn: Dr. A. B. Amster,
Chemistry Division
China Lake, California 93555 1

Naval Civil Engineering Laboratory
Attn: Dr. R. W. Drisko
Port Hueneme, California 93401 1

Department of Physics & Chemistry
Naval Postgraduate School
Monterey, California 93940 1

Scientific Advisor
Commandant of the Marine Corps
(Code RD-1)
Washington, D.C. 20380 1

Naval Ship Research and Development
Center
Attn: Dr. G. Bosmajian, Applied
Chemistry Division
Annapolis, Maryland 21401 1

Naval Ocean Systems Center
Attn: Dr. S. Yamamoto, Marine
Sciences Division
San Diego, California 91232 1

Mr. John Boyle
Materials Branch
Naval Ship Engineering Center
Philadelphia, Pennsylvania 19112 1

TECHNICAL REPORT DISTRIBUTION LIST, 056

	No. Copies
Dr. S. Sibener Department of Chemistry James Franck Institute 5640 Ellis Avenue Chicago, Illinois 60637	1
Dr. M. G. Lagally Department of Metallurgical and Mining Engineering University of Wisconsin Madison, Wisconsin 53706	1
Dr. Robert Gomer Department of Chemistry James Franck Institute 5640 Ellis Avenue Chicago, Illinois 60637	1
Dr. R. G. Wallis Department of Physics University of California, Irvine Irvine, California 92664	1
Dr. D. Ramaker Chemistry Department George Washington University Washington, D.C. 20052	1
Dr. P. Hansma Chemistry Department University of California, Santa Barbara Santa Barbara, California 93106	1
Dr. P. Hendra Chemistry Department Southampton University England SO9JNH	1
Professor P. Skell Chemistry Department Pennsylvania State University University Park, Pennsylvania 16802	1
Dr. J. C. Hemminger Chemistry Department University of California, Irvine Irvine, California 92717	1

	No. Copies
Dr. Martin Fleischmann Department of Chemistry Southampton University Southampton SO9 5NH Hampshire, England	1
Dr. J. Osteryoung Chemistry Department State University of New York at Buffalo Buffalo, New York 14214	1
Dr. G. Rubloff I.B.M. Thomas J. Watson Research Center P. O. Box 218 Yorktown Heights, New York 10598	1
Dr. J. A. Gardner Department of Physics Oregon State University Corvallis, Oregon 97331	1
Dr. G. D. Stein Mechanical Engineering Department Northwestern University Evanston, Illinois 60201	1
Dr. K. G. Spears Chemistry Department Northwestern University Evanston, Illinois 60201	1
Dr. R. W. Plummer University of Pennsylvania Department of Physics Philadelphia, Pennsylvania 19104	1
Dr. E. Yeager Department of Chemistry Case Western Reserve University Cleveland, Ohio 41106	2
Professor D. Hercules University of Pittsburgh Chemistry Department Pittsburgh, Pennsylvania 15260	1

TECHNICAL REPORT DISTRIBUTION LIST, 056

	No. Copies
Dr. G. A. Somorjai Department of Chemistry University of California Berkeley, California 94720	1
Dr. L. N. Jarvis Surface Chemistry Division 4555 Overlook Avenue, S.W. Washington, D.C. 20375	1
Dr. J. B. Hudson Materials Division Rensselaer Polytechnic Institute Troy, New York 12181	1
Dr. John T. Yates Department of Chemistry University of Pittsburgh Pittsburgh, Pennsylvania 15260	1
Dr. Theodore E. Madey Surface Chemistry Section Department of Commerce National Bureau of Standards Washington, D.C. 20234	1
Dr. J. M. White Department of Chemistry University of Texas Austin, Texas 78712	1
Dr. Keith H. Johnson Department of Metallurgy and Materials Science Massachusetts Institute of Technology Cambridge, Massachusetts 02139	1
Dr. J. E. Demuth IBM Corportion Thomas J. Watson Research Center P.O. Box 218 Yorktown Heights, New York 10598	1
Dr. C. P. Flynn Department of Physics University of Illinois Urbana, Illinois 61801	1
Dr. W. Kohn Department of Physics University of California (San Diego) LaJolla, California 92037	1
Dr. R. L. Park Director, Center of Materials Research University of Maryland College Park, Maryland 20742	1
Dr. W. T. Peria Electrical Engineering Department University of Minnesota Minneapolis, Minnesota 55455	1
Dr. Chia-wei Woo Department of Physics Northwestern University Evanston, Illinois 60201	1
Dr. D. C. Mattis Polytechnic Institute of New York 333 Jay Street Brooklyn, New York 11201	1
Dr. Robert M. Hexter Department of Chemistry University of Minnesota Minneapolis, Minnesota 55455	1
Dr. R. P. Van Duyne Chemistry Department Northwestern University Evanston, Illinois 60201	1

TECHNICAL REPORT DISTRIBUTION LIST, 056

No.
Copies

Professor N. Winograd
The Pennsylvania State University
Department of Chemistry
University Park, Pennsylvania 16802 1

Professor T. F. George
The University of Rochester
Chemistry Department
Rochester, New York 14627 1

Professor Dudley R. Herschbach
Harvard College
Office for Research Contracts
1350 Massachusetts Avenue
Cambridge, Massachusetts 02138 1

Professor Horia Metiu
University of California,
Santa Barbara
Chemistry Department
Santa Barbara, California 93106 1

Professor A. Steckl
Rensselaer Polytechnic Institute
Department of Electrical and
Systems Engineering
Integrated Circuits Laboratories
Troy, New York 12181 1

Professor R. D. Archer
University of Massachusetts
Chemistry Department
Amherst, Massachusetts 01003 1

Dr. A. C. Pastor
Hughes Research Laboratories
3011 Malibu Canyon Road
Malibu, California 90265 1

END

DATE
FILMED

5-82

DTIC